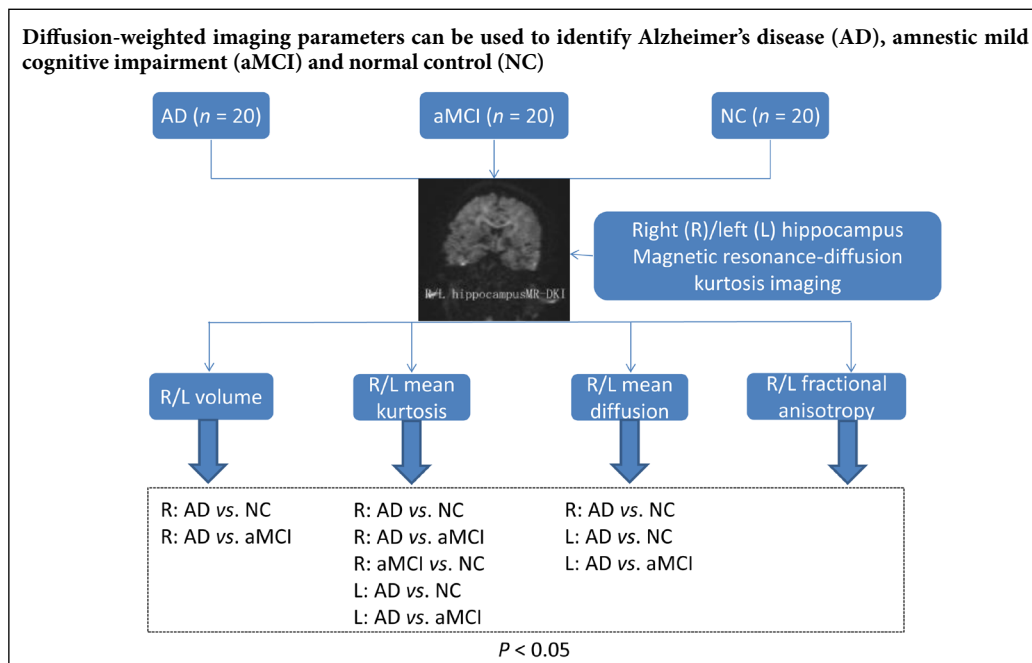# Differentiating between Alzheimer's disease, amnestic mild cognitive impairment, and normal aging *via* diffusion kurtosis imaging

Guo-Ping Song[#], Ting-Ting Yao[#], Dan Wang, Yue-Hua Li[*]

Institute of Diagnostic and Interventional Radiology, Affiliated Sixth People's Hospital of Shanghai Jiao Tong University, Shanghai, China

Graphical Abstract

Diffusion-weighted imaging parameters can be used to identify Alzheimer's disease (AD), amnestic mild cognitive impairment (aMCI) and normal control (NC)

Correspondence to:
Yue-Hua Li, PhD, MD,
liyuehua312@163.com.

#Both authors contributed equally to this article.

orcid:
0000-0001-8028-248X
(Yue-Hua Li)

Abstract

Diffusion kurtosis imaging can be used to assess pathophysiological changes in tissue structure and to diagnose central nervous system diseases. However, its sensitivity in assessing hippocampal differences between patients with Alzheimer's disease and those with amnestic mild cognitive impairment has not been characterized. Here, we examined 20 individuals with Alzheimer's disease (11 men and 9 women, mean 73.2 ± 4.49 years), 20 with amnestic mild cognitive impairment (10 men and 10 women, mean 71.55 ± 4.77 years), and 20 normal controls (11 men and 9 women, mean 70.45 ± 5.04 years). We conducted diffusion kurtosis imaging, using a 3.0 T magnetic resonance scanner, to compare hippocampal differences among the three groups. The results demonstrated that the right hippocampal volume and bilateral mean kurtosis were remarkably smaller in individuals with Alzheimer's disease compared with those with amnestic mild cognitive impairment and normal controls. Further, the mean kurtosis was lower in the amnestic mild cognitive impairment group compared with the normal control group. The mean diffusion in the left hippocampus was lower in the Alzheimer's disease group than in the amnestic mild cognitive impairment and normal control groups, while the mean diffusion in the right hippocampus was lower in the Alzheimer's disease group than in the normal control group. Fractional anisotropy was similar among the three groups. These results verify that bilateral mean kurtosis and mean diffusion are sensitive to the diagnosis of Alzheimer's disease and amnestic mild cognitive impairment. This study was approved by the Ethics Review Board of Affiliated Sixth People's Hospital of Shanghai Jiao Tong University, China on May 4, 2010 (approval No. 2010(C)-6).

Key Words: nerve regeneration; magnetic resonance imaging; diffusion kurtosis imaging; hippocampus; amnestic mild cognitive impairment; Alzheimer's disease; mean kurtosis; mean diffusion; fractional anisotropy; neural regeneration

Chinese Library Classification No. R445; R339.3+8; R741

Introduction

Alzheimer's disease (AD) is the most common cause of senile dementia (Harris et al., 1998). The characterization of amnestic mild cognitive impairment (aMCI) is important in the diagnosis of AD. Annually, approximately 15% of aMCI patients develop AD, and over a period of 7 years, 80% will develop AD (Bruegel et al., 2009). Modern neuroimaging techniques can aid the diagnosis of AD, particularly for aMCI patients (Harris et al., 1998; Bruegel et al., 2009).

Diffusion tensor imaging was derived from diffusion-weighted imaging technology. Although some scholars have used diffusion tensor imaging in the study of AD (Zhang et al., 2007; Mielke et al., 2009; Stebbins and Murphy, 2009; Wang et al., 2009), the scope of application is limited with respect to white matter (Li et al., 2017). Diffusion kurtosis imaging is based on a technical extension of diffusion tensor imaging. This new form of magnetic resonance imaging can be used to describe non-Gaussian water diffusion behavior (Wu and Cheung, 2010). The Gaussian distribution of free water diffusion is not sufficient to describe diffusion in biological environment. Most complex structures in human tissue, such as various types of cells, cell membranes, and the biochemical properties of such tissue, exhibit Gaussian diffusion that has a non-Gaussian distribution.

To describe this non-Gaussian diffusion behavior, kurtosis was introduced as the fourth tensor of distribution (Wu and Cheung, 2010). Physiological and biochemical status not only affects the diffusion rate of water molecules, but also influences water dispersion characteristics in different directions. Diffusion kurtosis imaging can be used to evaluate changes in the pathophysiology of the organizational structure, and thus has great potential in the diagnosis of central nervous system diseases. For instance, diffusion kurtosis imaging can be used as an indicator of tissue complexity, including gray matter and white matter (Jensen et al., 2005; Hui et al., 2008), and has been assessed for its potential in the early diagnosis of AD (Falangola et al., 2013; Gong et al., 2013; Struyfs et al., 2015; Wang et al., 2015; Yuan et al., 2016). The sensitivity of diffusion kurtosis imaging in assessing hippocampal differences between aMCI and AD patients has not been comprehensively investigated. Thus, in this exploratory study, we used diffusion kurtosis imaging to assess differences between individuals with aMCI, AD, and normal volunteers.

Participants and Methods

Participants

Written informed consent (**Additional file 1**) was obtained from the volunteers or their guardians before conducting magnetic resonance imaging scanning. This was a cross-sectional study. The study protocol was reviewed and approved by the Ethics Review Board of our Hospital (approval No. 2010(C)-6; **Additional file 2**) on May 4, 2010. The study conformed to the 2013 WMA *Declaration of Helsinki*. This trial has been registered in the ISRCTN Registry (IS-RCTN17337128).

The AD group was diagnosed in accordance with the following criteria (McKhann et al., 1984): (1) the criteria of the Diagnostic and Statistical Manual of Mental Disorders IV and the National Institute of Neurological and Communicative Disorders and Stroke/Alzheimer's Disease and Related Disorders Association; (2) a mini-mental state examination score of ≤ 23.

The Petersen diagnostic criteria were used to identify cases of aMCI (Petersen, 2004) according to (1) complaints of memory impairment confirmed by others; (2) objective evidence of memory impairment, *e.g.*, memory test (delayed story recall test) scores lower than (age- and duration-) matched healthy controls by 1.5 standard deviations; (3) an overall normal level of cognitive function, that is, insufficient impairment for dementia diagnosis, Clinical Dementia Rating scale point = 0.5; and (4) normal daily living skills according to the Activities of Daily Living scale, with a mini-mental state examination score of < 26 points.

In the normal control (NC) group, the inclusion criteria included the capacity for independence, normal neurological examination results, and a mini-mental state examination score of ≥ 28 points.

Two neurologists with 8 and 10 years of work experience, respectively, made all diagnoses. The mini-mental state examination (Tombaugh and McIntyre, 1992) is an extensively used global assessment tool with identification and tracking features. All subjects were right-handed, with no history of hypertension, diabetes, mental illness, cancer, autoimmune or other diseases, or alcohol/drug abuse. For the AD and aMCI groups, we required the Hachinski Ischemic Scale scores (Hachinski et al., 2012) to be less than 4, thus excluding participants with vascular cognitive impairment and vascular dementia.

Three subjects with AD and one subject with aMCI were excluded from the analysis because of excessive motion artifacts. As a result, 20 subjects with AD, 20 subjects with aMCI, and 20 NC subjects were included in the final analysis. There were no significant differences in age, sex, or education level among the three groups (*P* > 0.05; **Table 1**). The study flow chart is shown in **Figure 1**. This study followed the Strengthening the Reporting of Observational Studies in Epidemiology (STROBE) guidance (**Additional file 3**).

Magnetic resonance examination and measurement

We used a 3.0 T magnetic resonance scanner (MAGETOM, Verio, Siemens Healthcare, Erlangen, Germany) with a

Table 1 Differences in age, sex, years of education, and MMSE scores among the NC, aMCI, and AD groups

Item	NC	aMCI	AD
Age (year)	70.45±5.04	71.55±4.77	73.2±4.49
Sex ratio (male: female)	1.22	1	1.22
Years of education	8.24±3.84	6.06±4.14	9.54±6.75
MMSE score	29.22±0.97	26.85±1. 42*	21.15 ±1.23##

Data are expressed as the mean ± SD (*n* = 20; one-way analysis of variance and Fisher test). *P* < 0.05, *vs.* NC group; #P < 0.05, *vs.* aMCI group. MMSE: Mini-mental state examination; NC: normal control; aMCI: amnestic mild cognitive impairment; AD: Alzheimer's disease.

32-channel head coil. The imaging sequences included conventional magnetic resonance sequences (T1-weighted imaging, T2-weighted imaging), diffusion-weighted imaging, and diffusion kurtosis imaging sequences. The imaging parameters were as follows. For T2 images: field of view, 250 mm; repetition time/echo time, 6000/95 ms. For T1 3D axial images: field of view, 230 mm; repetition time/echo time, 1500/2.96 ms. The slice thickness was 1 mm for both T2 and T1 3D images.

We conducted diffusion kurtosis imaging in all subjects using 30 gradient directions, six *b* values (the diffusion sensitive gradient value) (b = 0, 500, 1000, 1500, 2000, and 2500 s/mm^2), and an echo-planar diffusion-weighted imaging sequence (**Figure 2**). Parametric maps for mean diffusion and mean kurtosis were generated using in-house MatLab code from the raw diffusion images and calculated using MRIcron software (http://www.nitrc.org/projects/mricron).

To measure hippocampal volume, we acquired oblique coronal images parallel to the brainstem from the T1-weighted axial images. On a Siemens workstation, two neuroradiologists (with 5 and 8 years of experience, respectively) manually outlined the hippocampus on the T1-weighted images. Each hippocampus was manually traced using multiple views of each layer to include the cornu ammonis, gyrus dentatus, and subiculum (the hippocampus is bordered by the temporal horn of the lateral ventricle, amygdala, and splenium). The neuroradiologists also measured the mean diffusion and mean kurtosis values of the hippocampus based on the mean diffusion and mean kurtosis images. Using MRIcron software to refer to different parameter maps in a brain atlas, the region of interest, that is, the hippocampus, was manually depicted on continuous sections. This was conducted to avoid manual editing errors, which may introduce bias into the analyses. We then subjected the data to a quality control step, in which values that exceeded the scope of the mean plus or minus three times the standard deviation were excluded from further analysis.

The hippocampus was segmented on the basis of anatomical boundaries, as described by MacMaster et al. (2008). The hippocampus volume was adjusted for intracranial volume using the covariance method, with the equation Va = Vua – G · (Vsic – Vmic), where Va is the adjusted volume; Vua is the unadjusted volume; G is the gradient; Vsic is the subject's intracranial volume; and Vmic is the mean intracranial volume for all control subjects. The variable gradient was derived by regressing the unadjusted volumes against the intracranial volumes across all subjects. Intracranial volumes were obtained *via* a previously validated approach, that is, the atlas scaling factor in the Freesurfer program in MRIcron software.

Statistical analysis
We used SPSS 19.0 (IBM, Armonk, NY, USA) for statistical analysis. We used a one-way analysis of variance to compare differences in the bilateral mean kurtosis, mean diffusion values, and volumes of the hippocampus among the three groups with Fisher's least significant difference test. Fisher's test was also applied for comparisons between two groups.

We chose an alpha level of 0.05.

Results

Normalized hippocampal volume among the aMCI, AD, and NC groups

With regards to normalized hippocampal volume, there were no significant differences between the aMCI and NC groups in the right or left hemispheres (P = 0.22214 and 0.08269, respectively; **Table 2**, **Figures 3** and **4**).

Table 2 Normalized hippocampal volumes (cm^3) among aMCI, AD, and NC groups

	NC	aMCI	AD
Right hippocampus	2.74±0.38	2.61±0.35	2.10±0.32[#]
Left hippocampus	2.62±0.51	2.35±0.47	2.05±0.45

Data are expressed as the mean ± SD (n = 20; one-way analysis of variance followed by Fisher's least significant difference test). #P < 0.05, *vs*. aMCI group. NC: Normal control; aMCI: amnestic mild cognitive impairment; AD: Alzheimer's disease.

Mean kurtosis and mean diffusion among the aMCI, AD, and NC groups

The mean kurtosis in the left and right hippocampi was lower in the AD group than in the aMCI and NC groups. We found significant differences in mean kurtosis between the NC and aMCI groups, the AD and NC groups, and the AD and aMCI groups in the left hemisphere (P = 0.004, < 0.001, and 0.029, respectively; **Table 3**, **Figures 3** and **4**). Among the three groups, the mean kurtosis values were lowest in the AD group. There was a significant difference in the mean diffusion values in the hippocampus between the AD and NC groups in the right hemisphere (P < 0.001). There were also significant differences between the AD and NC groups and between the AD and aMCI groups in the left hemisphere (P = 0.0211 and 0.027, respectively; **Figures 3** and **4**). Among the three groups, the mean diffusion values were highest in the AD group. We found no significant differences in fractional anisotropy among the three groups (**Table 3**).

Table 3 Mean kurtosis, mean diffusion, and fractional anisotropy values in the bilateral hippocampi among the NC, aMCI, and AD groups

	NC	aMCI	AD
Mean kurtosis			
Right hippocampus	0.81±0.20	0.70±0.09[*]	0.59±0.10[*#]
Left hippocampus	0.79±0.08	0.69±0.09	0.61±0.14[*#]
Mean diffusion			
Right hippocampus	1.34±0.30	1.47±0.20	1.60±0.18[*]
Left hippocampus	1.13±0.26	1.14±0.29	1.36±0.35[*#]
Fractional anisotropy			
Right hippocampus	0.17±0.05	0.17±0.03	0.16±0.02
Left hippocampus	0.18±0.05	0.17±0.04	0.16±0.03

Data are expressed as the mean ± SD (n = 20; analysis of variance followed by the Fisher's least significant difference test). *P < 0.05, *v*s. NC group; #P < 0.05, *v*s. aMCI group. NC: Normal control; aMCI: amnestic mild cognitive impairment; AD: Alzheimer's disease.
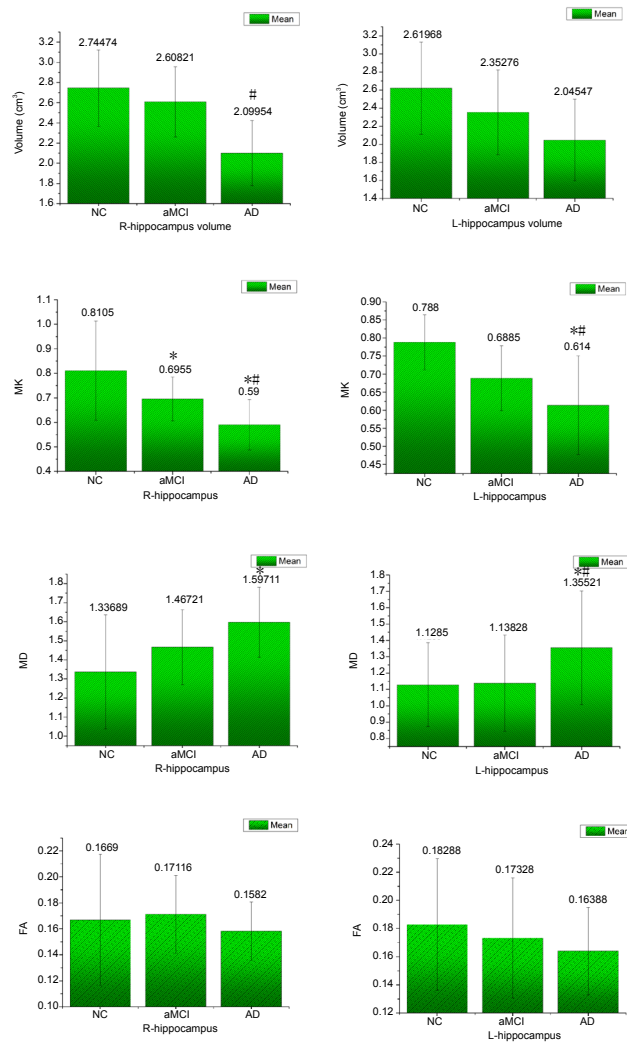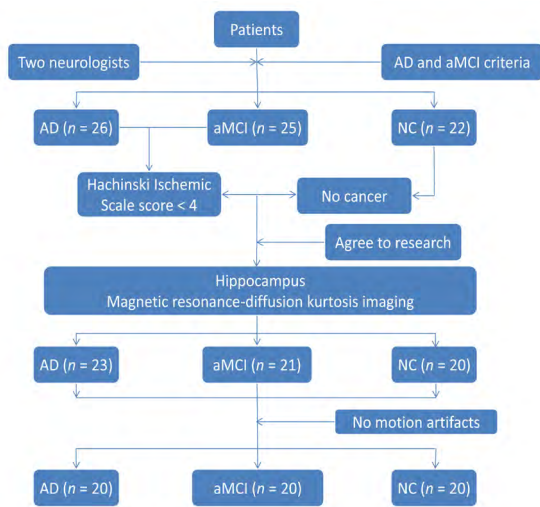
Figure 1 Trial flow chart.
NC: Normal control; aMCI: amnestic mild cognitive impairment; AD: Alzheimer's disease.
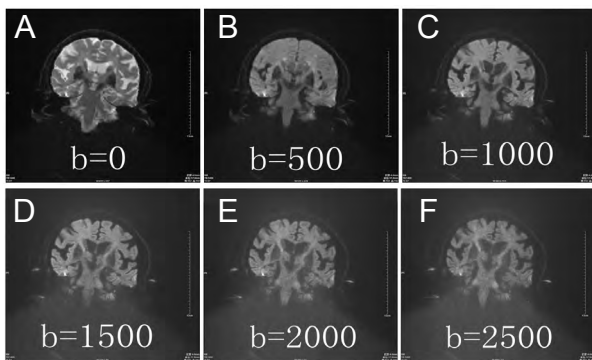
Figure 2 Diffusion kurtosis imaging of a 67-year-old male patient with Alzheimer's disease.
Diffusion kurtosis imaging was conducted parallel to brainstem oblique coronal images. (A–F) b = 0, 500, 1000, 1500, 2000, and 2500, respectively.

Figure 3 MK, MD, and FA values of bilateral hippocampal volume in the aMCI, AD, and NC groups.
Data are expressed as the mean ± SD (n = 20; analysis of variance followed by Fisher's least significant difference test). *P < 0.05, vs. NC group; #P < 0.05, vs. aMCI group. NC: Normal control; aMCI: amnestic mild cognitive impairment; AD: Alzheimer's disease; MK: mean kurtosis; MD: mean diffusion; FA: fractional anisotropy; R: right; L: left.
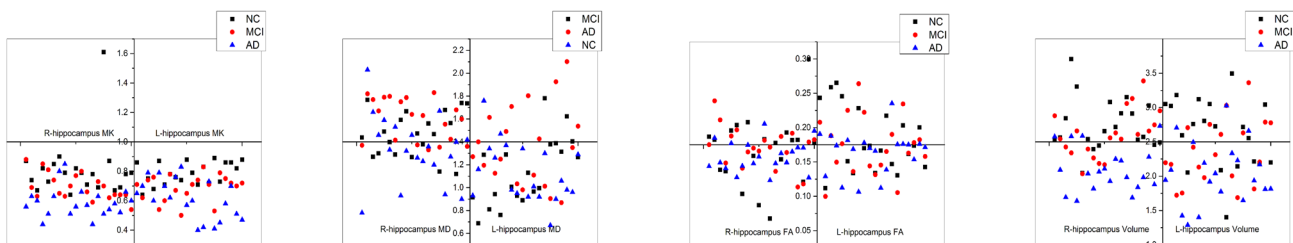
Figure 4 Distribution plots of MK, MD, FA, and volume of the bilateral hippocampi in the aMCI, AD, and NC groups.
MK: Mean kurtosis; MD: mean diffusion; FA: fractional anisotropy; NC: normal control; aMCI: amnestic mild cognitive impairment; AD: Alzheimer's disease; R: right; L: left.

Discussion

Diffusional non-Gaussianity is the result of diffusive barriers and compartments in tissue structures. Mean kurtosis value can reflect the non-Gaussianity of water molecule, and mean kurtosis value can reflect the micro-change of water molecule (Jensen and Helpern, 2010). The mean kurtosis value of the probability distribution of diffusion displacement can be determined from a diffusion kurtosis imaging dataset. This has potential practical value in characterizing changes in brain tissue induced by neuropathology (including AD) (Jensen et al., 2005; Jensen and Helpern, 2010).

Mean kurtosis values rely on the structural complexity of the region of interest. Structures with greater complexity have more visible non-Gaussian water molecule diffusion, and thus higher mean kurtosis values. Although we found that aMCI hippocampal volume was not substantially reduced compared with the NCs, the associated pathological changes in neurons, including degeneration, apoptosis, and demyelination, all lead to a decrease in cell complexity (Juottonen et al., 1999; Jensen and Helpern, 2010). While this coincides with the expansion of extracellular space and compensatory glial cells (Juottonen et al., 1999), glial cells are much less complex than neurons, leading to a clear decrease in mean kurtosis values. Consistent with previous studies, Grinberg et al. (2011) found that mean kurtosis values in the frontal cortex increased from adolescence to adulthood. Increases in mean kurtosis are associated with enhanced organizational structural complexity in the brain. However, age-related neurodegeneration, in terms of the microscopic structure of the whole brain, is accelerated in AD patients (Grinberg et al., 2011). Thus, microscopic changes lead to a decrease in mean kurtosis values. Mean kurtosis values (as measured in the present study) are considered to be a complex micro index. The advantage of mean kurtosis over fractional anisotropy is that the former does not depend on the spatial orientation of the organizational structure; both gray and white matter structures in the brain can be described using mean kurtosis. Fractional anisotropy measures the main characteristics of white matter fiber anisotropy parameters. Fractional anisotropy is strongly associated with the size and integrity of myelin, as well as fiber density and parallelism. Consistent with a previous study (Nakaaki et al., 2013), our results confirm that fractional anisotropy is not particularly advantageous in the evaluation of the hippocampal structure.

The hippocampus is closely linked with learning and memory, especially remote memory, and the transformation of memories from recent to remote storage functions. It is also one of the brain regions that is most likely to be affected by AD brain lesions. This is why we chose the hippocampus as the region of interest in the present study. Limited scanning time prevented us from examining other regions implicated in AD brain lesions, such as the frontal and temporal cortices.

In this study, we found asymmetry between the right and left hippocampi in the NCs, reflected by the mean diffusion value. Indeed, the internal structure of the hippocampus is asymmetric. However, studies of hippocampal asymmetry have mainly focused on animals. Dua et al. (2011a, 2011b) reported on internal hippocampal asymmetry in terms of the number of neurons. In addition to asymmetrical hippocampal morphology, asymmetric expression of proteins and other molecules has been recently proposed. Some researchers used proteomics and genomics to study differences between the rat right and left hippocampi. They found that hippocampal activation during the water maze performance varied such that the left hippocampus was dominant in the encoding and information transferring stage, and the right hippocampus was dominant in the memory compensation stage (Dua et al., 2011a, b). Mean diffusion in the brain mainly reflects the diffusion coefficient of water molecules, which is mainly determined by the sizes and number of cells inside and outside the defined cellular space. Whether the asymmetry of the hippocampal formation is reflected in the differences in the mean diffusion values between the right and left hippocampi remains unclear.

Although many researchers have used diffusion kurtosis imaging and diffusion tensor imaging to examine individuals with AD and mild cognitive impairment, none have reported a direct relationship between diffusion kurtosis imaging and diffusion tensor imaging. Consequently, further diffusion kurtosis imaging studies in animals and humans with large sample sizes are needed to ascertain the link between diffusion kurtosis imaging measurements and structural changes in AD and mild cognitive impairment.

Using the diffusion kurtosis imaging technique, we were able to distinguish AD patients, aMCI patients, and NC participants. Thus, mean kurtosis and mean diffusion values acquired using diffusion kurtosis imaging may be valuable in the diagnosis of aMCI and AD.

References

Bruegel M, Planert M, Baumann S, Focke A, Bergh FT, Leichtle A, Ceglarek U, Thiery J, Fiedler GM (2009) Standardized peptidome profiling of human cerebrospinal fluid by magnetic bead separation and matrix-assisted laser desorption/ionization time-of-flight mass spectrometry. J Proteomics 72:608-615.

Dua SG, Purandare NC, Shah S, Rangarajan V (2011a) F-18 fluoride PET/CT in the detection of radiation-induced pelvic insufficiency fractures. Clin Nucl Med 36:e146-149.

Dua SG, Shah S, Purandare NC, Arora B, Rangarajan V (2011b) Fibrodysplasia ossificans progressiva detected on FDG PET/CT. Clin Nucl Med 36:952-954.

Falangola MF, Jensen JH, Tabesh A, Hu C, Deardorff RL, Babb JS, Ferris S, Helpern JA (2013) Non-Gaussian diffusion MRI assessment of brain microstructure in mild cognitive impairment and Alzheimer's disease. Magn Reson Imaging 31:840-846.

Gong NJ, Wong CS, Chan CC, Leung LM, Chu YC (2013) Correlations between microstructural alterations and severity of cognitive deficiency in Alzheimer's disease and mild cognitive impairment: a diffusional kurtosis imaging study. Magn Reson Imaging 31:688-694.

Grinberg F, Farrher E, Kaffanke J, Oros-Peusquens AM, Shah NJ (2011) Non-Gaussian diffusion in human brain tissue at high b-factors as examined by a combined diffusion kurtosis and biexponential diffusion tensor analysis. Neuroimage 57:1087-1102.

Hachinski V, Oveisgharan S, Romney AK, Shankle WR (2012) Optimizing the Hachinski Ischemic Scale. Arch Neurol 69:169-175.

Harris GJ, Lewis RF, Satlin A, English CD, Scott TM, Yurgelun-Todd DA, Renshaw PF (1998) Dynamic susceptibility contrast MR imaging of regional cerebral blood volume in Alzheimer disease: a promising alternative to nuclear medicine. AJNR Am J Neuroradiol 19:1727-1732.

Hui ES, Cheung MM, Qi L, Wu EX (2008) Advanced MR diffusion characterization of neural tissue using directional diffusion kurtosis analysis. Conf Proc IEEE Eng Med Biol Soc 2008:3941-3944.

Jensen JH, Helpern JA (2010) MRI quantification of non-Gaussian water diffusion by kurtosis analysis. NMR Biomed 23:698-710.

Jensen JH, Helpern JA, Ramani A, Lu H, Kaczynski K (2005) Diffusional kurtosis imaging: the quantification of non-gaussian water diffusion by means of magnetic resonance imaging. Magn Reson Med 53:1432-1440.

Juottonen K, Laakso MP, Partanen K, Soininen H (1999) Comparative MR analysis of the entorhinal cortex and hippocampus in diagnosing Alzheimer disease. AJNR Am J Neuroradiol 20:139-144.

Li HX, Feng X, Wang Q, Dong X, Yu M, Tu WJ (2017) Diffusion tensor imaging assesses white matter injury in neonates with hypoxic-ischemic encephalopathy. Neural Regen Res 12:603-609.

MacMaster FP, Mirza Y, Szeszko PR, Kmiecik LE, Easter PC, Taormina SP, Lynch M, Rose M, Moore GJ, Rosenberg DR (2008) Amygdala and hippocampal volumes in familial early onset major depressive disorder. Biol Psychiatry 63:385-390.

McKhann G, Drachman D, Folstein M, Katzman R, Price D, Stadlan EM (1984) Clinical diagnosis of Alzheimer's disease: report of the NINCDS-ADRDA Work Group under the auspices of Department of Health and Human Services Task Force on Alzheimer's Disease. Neurology 34:939-944.

Mielke MM, Kozauer NA, Chan KC, George M, Toroney J, Zerrate M, Bandeen-Roche K, Wang MC, Vanzijl P, Pekar JJ, Mori S, Lyketsos CG, Albert M (2009) Regionally-specific diffusion tensor imaging in mild cognitive impairment and Alzheimer's disease. Neuroimage 46:47-55.

Nakaaki S, Sato J, Torii K, Oka M, Negi A, Nakamae T, Narumoto J, Miyata J, Furukawa TA, Mimura M (2013) Decreased white matter integrity before the onset of delusions in patients with Alzheimer's disease: diffusion tensor imaging. Neuropsychiatr Dis Treat 9:25-29.

Petersen RC (2004) Mild cognitive impairment as a diagnostic entity. J Intern Med 256:183-194.

Stebbins GT, Murphy CM (2009) Diffusion tensor imaging in Alzheimer's disease and mild cognitive impairment. Behav Neurol 21:39-49.

Struyfs H, Van Hecke W, Veraart J, Sijbers J, Slaets S, De Belder M, Wuyts L, Peters B, Sleegers K, Robberecht C, Van Broeckhoven C, De Belder F, Parizel PM, Engelborghs S (2015) Diffusion kurtosis imaging: a possible MRI biomarker for AD diagnosis? J Alzheimers Dis 48:937-948.

Tombaugh TN, McIntyre NJ (1992) The mini-mental state examination: a comprehensive review. J Am Geriatr Soc 40:922-935.

Wang D, Guo ZH, Liu XH, Li YH, Wang H (2015) Examination of hippocampal differences between Alzheimer disease, amnestic mild cognitive impairment and normal aging: diffusion kurtosis. Curr Alzheimer Res 12:80-87.

Wang L, Goldstein FC, Veledar E, Levey AI, Lah JJ, Meltzer CC, Holder CA, Mao H (2009) Alterations in cortical thickness and white matter integrity in mild cognitive impairment measured by whole-brain cortical thickness mapping and diffusion tensor imaging. AJNR Am J Neuroradiol 30:893-899.

Wu EX, Cheung MM (2010) MR diffusion kurtosis imaging for neural tissue characterization. NMR Biomed 23:836-848.

Yuan L, Sun M, Chen Y, Long M, Zhao X, Yin J, Yan X, Ji D, Ni H (2016) Non-Gaussian diffusion alterations on diffusion kurtosis imaging in patients with early Alzheimer's disease. Neurosci Lett 616:11-18.

Zhang Y, Schuff N, Jahng GH, Bayne W, Mori S, Schad L, Mueller S, Du AT, Kramer JH, Yaffe K, Chui H, Jagust WJ, Miller BL, Weiner MW (2007) Diffusion tensor imaging of cingulum fibers in mild cognitive impairment and Alzheimer disease. Neurology 68:13-19.